Triple Band-stop Performance Realization Through a Single Substrate Layer Frequency Selective Surface

V. Nadjari[1], J. Nourinia[1], Ch. Ghobadi[1]
[1]Department of Electrical Engineering, Urmia University, Urmia, Iran

Corresponding author: V. Nadjari (e-mail: v.nadjari@urmia.ac.ir).

ABSTRACT A single-substrate-layer Frequency Selective Surface (FSS) is designed with a 1.6 mm thick FR4 substrate for triple band-stop frequency filtering applications, that are for Bluetooth, WLAN, WiMAX, and X-band. The proposed FSS unit cell consists of two polygon loops on the front side and a square loop with four annular rings attached to its corners on the backside. The offered design covers three frequency bands: 2.3-4 GHz, 5-6 GHz, and 8-12 GHz. There are three resonances at 3.3 GHz, 5.6 GHz, and 9.9 GHz. The equivalent circuit model of the proposed structure and the formulas of the LC parameters were presented. A prototype of this structure was manufactured in size of 26 cm × 26 cm and experimentally verified in the antenna and microwave laboratory. The software used for design and simulation is HFSS from Ansys, which uses the finite element method. A comparison with similar structures was performed to demonstrate the performance of the proposed structure. The advantages of the proposed filter include adequate bandwidth, simple structure, as well as small size. In addition, it is unaffected by variant angles of incidence for TE polarization and TM polarization. Furthermore, due to its symmetrical design, it shows a polarization-independent feature. Experimental results for both polarizations verify the merits of the proposed approach, as shown before in the simulation results as well.

INDEX TERMS Frequency Selective Surfaces(FSS), Bluetooth, WLAN, WiMAX, X-band

I. INTRODUCTION

PERIODIC structures that encounter electromagnetic waves and act as filters, but are a function of frequency, called Frequency Selective Surfaces(FSS). FSSs are filters that result from the placement of several identical metal shapes together in a repetitive pattern printed on a substrate. According to their design, they can reject or pass electromagnetic waves radiated towards them. These electromagnetic filters can act as band-stop, band-pass, low-pass, and high-pass filters like microwave filters [1-3]. Perhaps the biggest problem of a periodic structure is that it conceptually is so simple that almost everyone understands it instantly. However, the designer soon realizes that one has to produce more than just some calculated curves [4]. FSSs have many advantages; however, there are some difficulties in designing and manufacturing them that need to be considered. These difficulties include the following [5]:

1) Large-size unit cells, the larger the cell, the larger the FSS;
2) Difficulties in achieving the desired band and specific frequency range;
3) Complex structures, which make FSS challenging to build;
4) The number of substrate layers.

Some of the FSSs main applications are in band-stop filters [6-9], dichroic subreflector [10], radomes [11], RCS reduction and absorbers [12]. It is noteworthy that a dichroic structure refers to a periodic surface that is clear at a frequency band and opaque at another.

Reference [13] proposed a left-handed metasurface absorber inspired by a tree-shaped fractal structure with tri-band (C-, X-, and Ku-bands) resonances. Each single unit cell contains a metallic branch tree-shaped fractal printed on a 1.6 mm thick epoxy resin fiber substrate. The absorption of the structure is above 84%. Reference [14] proposed a multilayered reconfigurable FSS using cantilever enable switches. The unit cell size is 10.1 mm × 7.62 mm. The arms of the top layer in this super-shape-inspired structure FSS, are used as cantilever switches. Depending on the bending of cantilever arms, this structure has two states (UP & DOWN); for UP state, the cantilever arms are bent, while for DOWN state, they are left unbend. The proposed structure is for X-band application and has good isolation between UP and DOWN states.

We all know that security against unwanted signals is one of the main concerns of some places today, which can be overcome by using the FSS signal blocking feature and using them as a band-stop filter. Reference [15] proposed a shielding structure using complementary frequency selective surfaces for EMI from LTE 4G systems. The geometry of the proposed unit cell is complementary, which includes a 16 mm square

loop and a cross-dipole. This structure resembles a filter with two transmission bands, the first at 2.11 GHz and the second at 3.11 GHz, with a null between them. It rejects the frequency band of 2.45-2.69 GHz, which includes 4G LTE band 7. Reference [16] designed textile-based FSSs to stop four different frequency bands, where EM pollution generally occurs. Four different FSSs named S1, S2, S3, and S4 are designed using textile material (felt, satin, jersey, and akfil-cotton, respectively). The geometry of proposed unit cells is H-shape patch for S1(65 mm × 20 mm), square patch for S2(60 mm × 30 mm), hexagon patch for S3(60 mm × 40 mm), and hexagon loop for S4(50 mm × 40 mm). The simulations show four resonances at 4.96 GHz, 4.5 GHz, 4.6 GHz, and 3.78 GHz respectively. It has been claimed that these FSSs are suitable for wearable antennas and sensors. Reference [17] designed a compact metamaterial antenna with a dimension of 42 mm × 32 mm for LTE, Bluetooth, and WiMAX system, using square metallic strips. The measured results of the conventional antenna show three resonances at 0.56 GHz, 2.67 GHz, and 3.15 GHz that cover the bandwidth of 20MHz (0.56-0.57 GHz), 560 MHz (2.326-2.9 GHz), and 580 MHz (2.91-3.49 GHz), whereas the metamaterial inspired antenna shows three resonances at 0.63 GHz, 3.21 GHz, and 3.63 GHz that covers the bandwidth of 40MHz (0.6-0.64 GHz), 730 MHz (2.67-3.4 GHz), and 60MHz (3.61-3.67 GHz). It has been claimed that the proposed antenna is a good choice for LTE and WiMAX applications because it has an Omni-directional radiation pattern with a high peak gain during the operating frequency band.

In this paper, the design procedure of a unit cell on a 10 mm × 10 mm FR4 substrate is explained in detail. The substrate is 1.6 mm thick and has a dielectric constant of 4.4. Design parameters such as substrate permittivity, cell size, cell shape, loss tangent, inter-element spacing have been conservatively considered in the design procedure to achieve an appropriate frequency response. These show how design considerations such as the proportionality among mentioned parameters help us to achieve the desired frequency. Proper selection of conductive elements has helped us to filter three bands from 2.3-4 GHz, 5-6 GHz, and 8-12 GHz, which include Bluetooth, WLAN, WiMAX, and X-band frequency bands. The symmetric structure has stable performance in dealing with waves with an oblique or direct angle of incidence for TM and TE wave modes. The proposed FSS is designed and analyzed firstly by Ansys HFSS software (finite-element method based) and then its performance is verified through an experimental prototype sample. The rest of the paper continues as follows: section 2 explains the process of designing the proposed unit cell. In section 3 the simulated and experimental results are presented and we investigate the sensitivity of the suggested FSS and the surface current distribution analysis. Section 4 examines a comparison between similar structures. At last, section 5 concludes the paper.

II. DESIGNING OF SINGLE CELL

Fig. 1 shows the unit cell of the suggested structure. It is developed on a 10 mm × 10 mm FR4 substrate that is 1.6 mm thick. For broadband applications, the FR4 can be used in place of conventional microwave substrates, offering significant cost savings and acceptable performance. It is low-cost, readily available, and satisfies our requirements based on the proposed structure. If we choose roger substrates based on the proposed design, the resonances shift to the higher frequencies, which in this case, it is not desired. Nevertheless, on the backside of the FR4 substrate, we printed a square loop with the outer and inner areas of 9.8 mm × 9.8 mm and 9.1 mm × 9.1 mm with four annular rings on the corners. The outer and inner diameter of the rings is 1.45 mm and 0.75 mm. The front side includes a hexagonal loop with a width of 0.85 mm in the wide part of the loop and 0.5 mm in the narrow part and

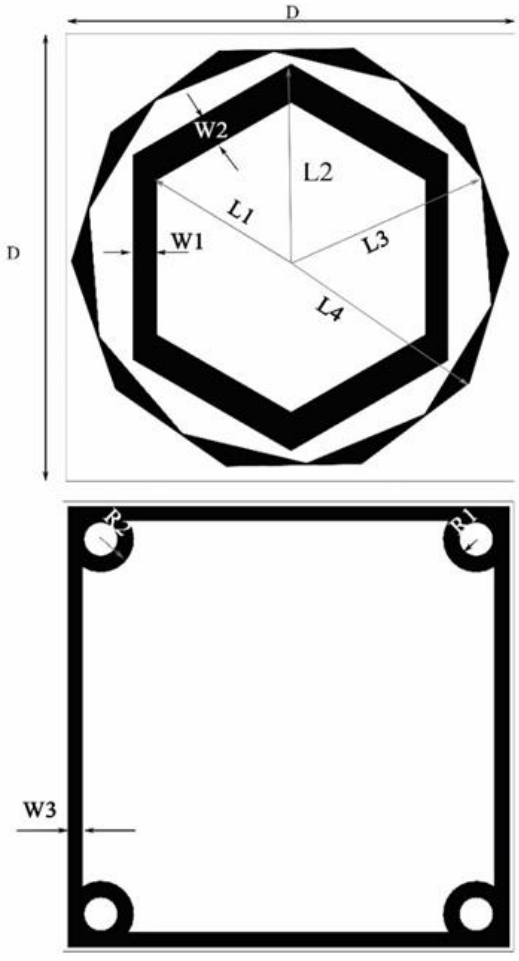

FIGURE 1. Proposed FSS unit cell dimensions.

an irregular decagonal loop. To have a thorough analysis, the procedure of developing the unit cell is completed in 4 steps. In step 1, all we can see is a simple square loop on the backside of the substrate. It stimulates a resonance around 3.1 GHz,

which rejects the frequency range of 2.1-4.4 GHz. As we know, loop-type elements are well known as band-stop filters. In step 2, we added a hexagonal loop to the front side. The addition of this element yields another resonance frequency around 10 GHz with a rejection band of 8.1-11.8 GHz and shifts the first resonance frequency from 3.1 GHz to 3.3 GHz. In the next step, an irregular decagonal loop that is made of two decagonal subtracted in simulation software has been supplemented on the front side of the substrate that creates a resonance around 5.6 GHz and filters the frequencies from 5 GHz to 6 GHz. Finally, in step 4, four annular rings are integrated into the corners of the square loop. Fig. 2 displays all four steps. For FSSs analysis, like other two-port networks, S-parameters will be useful to analyze their performances. S_{21} curves for all four steps are plotted in Fig. 3.

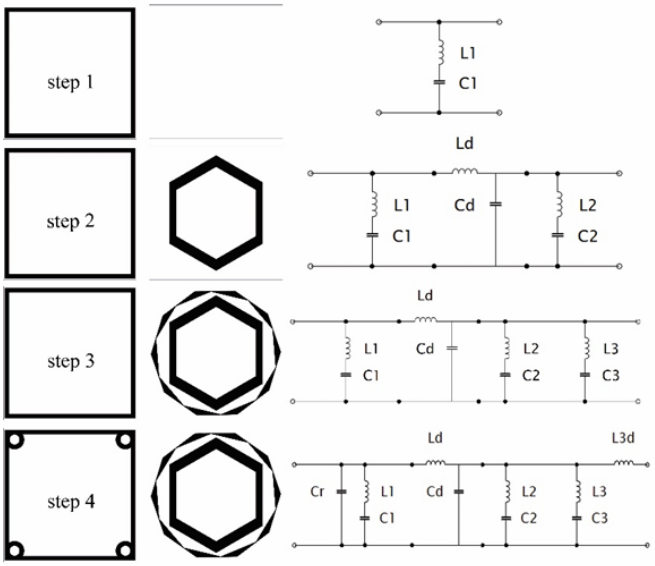

FIGURE 2. Unit cell design steps and Equivalent circuit model.

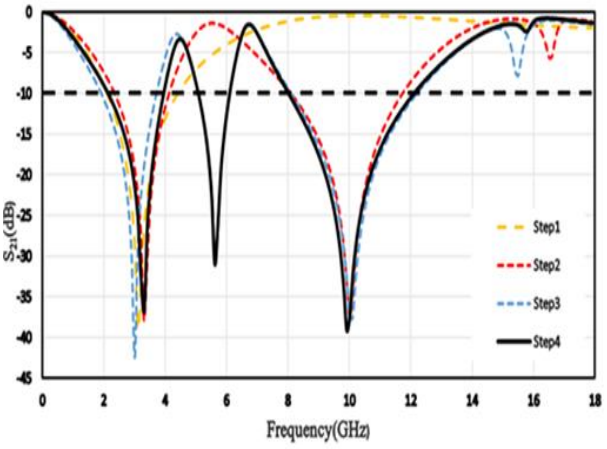

FIGURE 3. S_{21} curves for design steps.

TABLE I. *Dimensions of the FSS unit cell*

Parameter	Dimension(mm)	Parameter	Dimension(mm)
D	10	L_2	4.3
W_1	0.5	L_3	4.6
W_2	0.75	L_4	4.9
W_3	0.3	R_1	0.4
L_1	3.4	R_2	0.8

III. RESULTS AND DISCUSSION

A prototype of the FSS presented in this paper was manufactured and tested in the Urmia antenna and microwave laboratory. It has a 26 cm × 26 cm area, which contains a 26 × 26 array of unit cells at both sides. Fig. 5 shows an image of the FSS prototype. Two horn antennas with an operating frequency range of 2-18 GHz (on both sides of the prototype) are used to measure the prototype in the laboratory. These antennas have high gain and low VSWR. The benefits of having these antennas are maintaining a single main lobe pattern in the direction of the horn axis, uniform illumination of object planes, and precise measurement. The PNA network analyzer model is Agilent technology E8363C. To be able to simulate a quiet environment, we performed experiments in the Urmia Antenna and Microwave Laboratory in an echo-free room for TE polarization and TM polarization. Fig. 4(a) shows the established setup in the measurement process. To prevent spillover and diffraction, we surround the prototype with absorbent material. The results obtained by the experiment are shown in Fig. 4(b). As can be seen, the proposed FSS manifests three resonances at 3.3 GHz, 5.6 GHz, and 9.9 GHz. The rejected frequency ranges are from 2-3.4 GHz, 5-6 GHz, and 8-12 GHz, which include Satellite, SiriusXM Radio, unlicensed (Bluetooth, Wi-Fi, etc.), cellular phones, WiMAX, WLAN, and X-band in-service frequency ranges. The proposed structure can be used for electromagnetic shielding or utilize its unit cell in the filtenna systems. However, in upcoming works, we intend to employ the PIN diodes to turn this design into a tunable structure that can be used for both shielding applications and filtenna systems.

As can be seen from measured S_{21} curves for TE polarization, there is three main resonance frequency at 3.1 GHz, 5.5 GHz, and 9.8 GHz. Furthermore, the resonance frequencies for TM polarization are at 3.2 GHz, 5.6 GHz, and 9.8 GHz. The simulated and measured results are well conformant, as can be observed in Fig. 4(b).

Further discussions can be advanced by analyzing the equivalent circuit of the proposed structure. The double loop on the front side of the structure can be presented by two LC circuits. The short lengths of relatively high impedance lines behave mainly like a series inductor, so the discontinuity of

the irregular decagonal loop can be presented as a series inductor. The equivalent circuit model of the square loop is an LC circuit where inductance and capacitance are presented by vertical and horizontal metal conductors, respectively. The attached rings in the corners of the square loop create circular slots that raise the capacitance and shift the first resonance to the higher frequency. It can be modeled by a capacitor in parallel with the square loop. Also, the dielectric substrate is modeled by a series inductor(Ld) and a shunt capacitor (Cd). Fig. 2 shows the equivalent circuit of the presented FSS. The circular ring equations can be used for the inductance and capacitance of the irregular decagonal loop with a pretty good approximation. However, the inductance and capacitance of the structure can be obtained from the following equations [25-27]:

$$B_{C_1} = \varepsilon_{eff} Z_0 \frac{d_1}{p} F(p,g,\lambda). \quad (1)$$

$$X_{L_1} = \frac{4}{Z_0}\frac{d_1}{p} F(p,2W_1,\lambda). \quad (2)$$

$$B_{C_2'} = \varepsilon_{eff}\frac{1}{Z_0}\frac{8d_3}{p} F(p,g_2,\lambda). \quad (3)$$

$$X_{L_2} = Z_0\frac{d3}{p} F(p,\frac{d_2+d_3}{2},\lambda). \quad (4)$$

$$B_{C_3} = \varepsilon_{eff}\frac{\pi}{2}\frac{d_5}{p} 4F(p,g,\lambda). \quad (5)$$

$$X_{L_3} = \frac{\pi}{4}\frac{d_5}{p} F(p,2(\frac{d_4+d_5}{2}),\lambda). \quad (6)$$

$$X_2 = \frac{C_3 C_2'}{C_3 + C_2'}. \quad (7)$$

Where F is as follows:

$$F(p,W,\lambda) = \frac{p}{\lambda} Cos\theta[Ln(Co\sec\frac{\pi w}{2p}) + G(p,w,\lambda)]. \quad (8)$$

And G is:

$$G(p,w,\lambda) = \frac{1}{2}\frac{(1-\beta^2)[(1-\frac{\beta^2}{4})(A_+ + A_-) + 4\beta^2 A_+ A_-]}{(1-\frac{\beta^2}{4}) + \beta^2(1+\frac{\beta^2}{2}-\frac{\beta^4}{8})(A_+ + A_-) + 2\beta^6 A_+ A_-}. \quad (9)$$

In which:

$$A_{\pm} = \frac{1}{\sqrt{1 \pm \frac{2pSin\theta}{\lambda} - (\frac{pCos\theta}{\lambda})^2}} - 1. \quad (10)$$

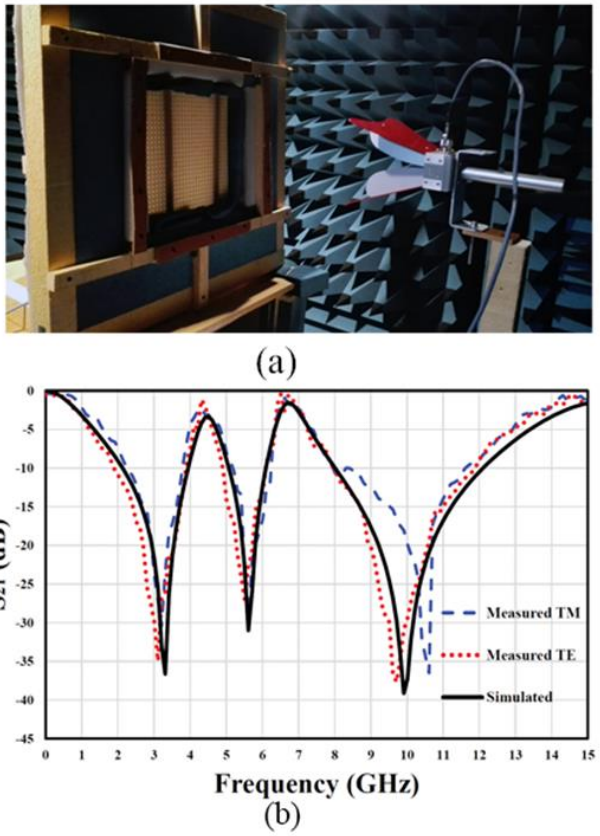

FIGURE 4. Antenna and microwave lab and testing the FSS, (a) Fabricated FSS under measurement (b) Simulated and measured S_{21} curves.

$$\beta = \frac{Sin\pi w}{2p}. \quad (11)$$

$$\varepsilon_{eff} = \varepsilon_r + (\varepsilon_r - 1)[\frac{-1}{\exp(x.N)}]. \quad (12)$$

Where

$$x = 10\frac{t}{p}. \quad (13)$$

The variables in the above equations can be defined as follows:

B_c: capacitive susceptance,

X_L: inductive reactance,

g : the gap between the loop sides, g_2: the gap between the two polygonal loops,

p: periodicity,

θ :angle of incidence,

λ: the wavelength,

t :the thickness of the substrate, and N is an exponential factor that varies with the geometry of the unit cell (N = 1.8 for loop arrays, N=1.3 for metal patches).

Eventually, the resonance frequency is achieved by the following formula:

$$f_r = \frac{1}{2\pi\sqrt{LC}}. \quad (14)$$

The calculated resonances from the above formulas are in 3.21 GHz, 5.49 GHz, and 9.86 GHz whereas, the simulated and the measured resonances are in 3.3 GHz, 5.6 GHz, 9.9 GHz, and 3.1 GHz, 5.5 GHz, 9.8 GHz, respectively.

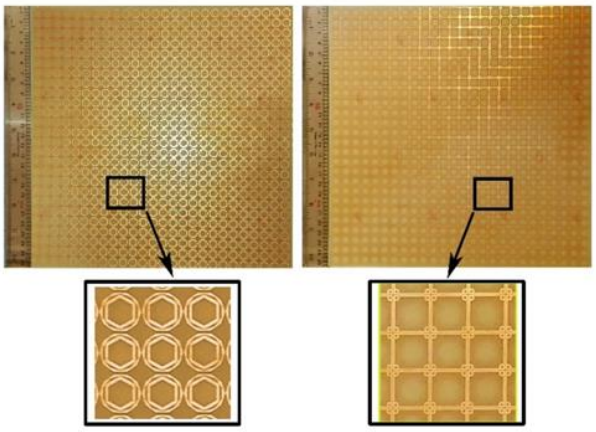

FIGURE 5. Fabricated prototype photograph.

A. SURFACE CURRENT

To inquire more into the FFS performance, surface current distribution analysis is employed. It designates the effect of the fields generated by the FSS sheet, at the resonant frequency. As we can see in Fig. 6, at 3.3 GHz, the surface current is centralized on the backside square loop. Red colors indicate a stronger current. At 5.6 GHz, the outer patch of the front side is excited most, and it is responsible for the resonance frequency. The last resonance occurs at 9.9 GHz. As shown in Fig. 6, the hexagonal loop is feverish, and therefore, it resonates at 9.9 GHz.

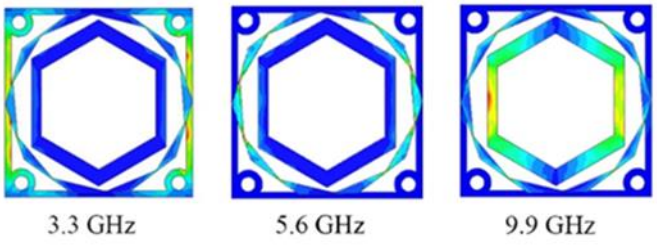

FIGURE 6. Surface current distribution at 3.3 GHz, 5.6 GHz, and 9.9 GHz.

B. SENSITIVITY

A favorable FSS requires a stable response and performance resistance to angles of incidence and different polarizations. For TE polarization and TM polarization and variant angles of incidence from 0° to 50°, S_{21} parameters are simulated, and a step change of 10° is employed. Fig. 7(a) and (b) shows the acquired S_{21} curves. It is clear that by increasing the angle of incidence from 0° to 50°, S_{21} has a slight shift, but it could be suitably neglected. Nevertheless, the overall response has frequency stability within the permitted boundary.

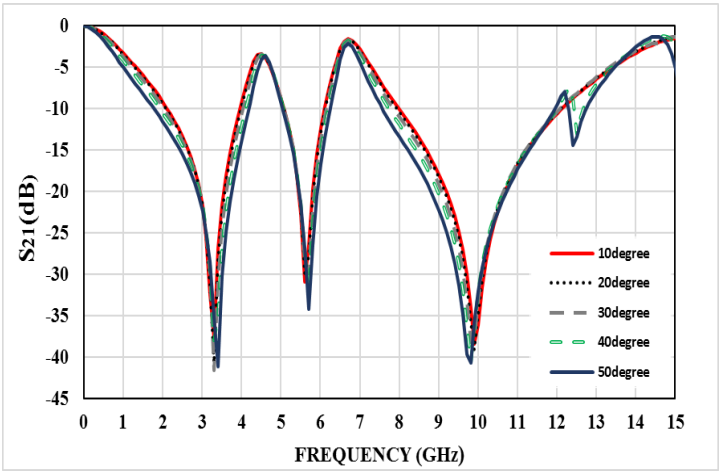

(a)

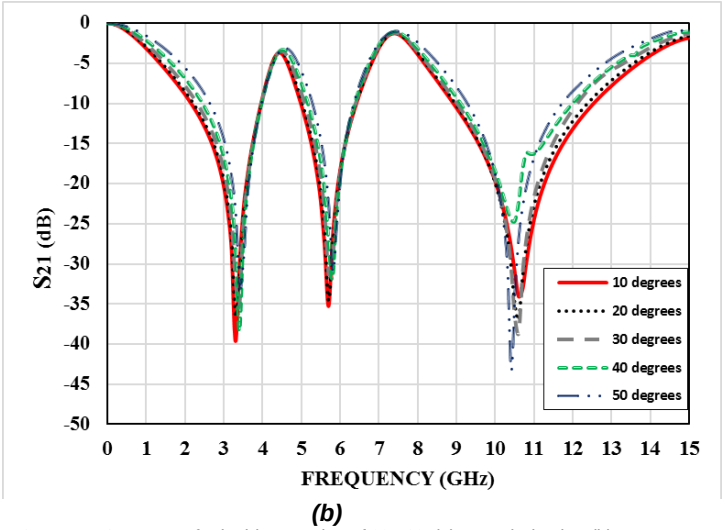

(b)

FIGURE 7. S_{21} curves for incident angles of 0°-50°, (a) TE polarization (b) TM polarization.

IV. COMPARISON

We performed a comparison with similar structures to understand the performance of the proposed structure better. The choice of structures for comparison is based on unit cell size, substrate type, and supported bands. As shown in Table II, the structures in [5], [7], [18], [19], [20], [21], [22], [23], and [24] are intended for comparison. All of the mentioned structures have been simulated and measured. Among these structures, only [5], [18], [22], [24], and the proposed structure

in this paper are multi-bands. Most of the selected structures for comparison have FR4 substrate except for [22] and [23], which have Rogers 4003c and F4BM220, respectively. The structures in [19] and [23] have two substrates layers. In terms of size, the structures in [5] and [7] and the structure presented in this paper are equal but not the smallest; however, the proposed FSS supports more frequency bands. [20] is the smallest among all and filters the 802.16e WiMAX, 802.11 WLAN, and Bluetooth good enough. [24] is a pentaband, single substrate, and larger than others, but only supports 802.16d WiMAX. [7] and [19] have wideband characteristics but fail to cover Bluetooth and all frequency range of WiMAX 802.16e. [18] is triple-band and covers WiMAX frequency bands well but fails to filter WLAN and X-band. Also, it should not be forgotten that its size is almost twice in comparison with the presented FSS. [5], [7] and [20] do not have symmetrical structures, so they are not polarization-independent. Generally, the structure proposed in this paper, despite its small size and single substrate, is three-band and succeeds in covering most of the considered frequencies.

V. CONCLUSION

In this article, a new scheme for frequency selective surfaces that filter the three frequency bands has been designed and experimentally verified, which include Bluetooth, WLAN, WiMAX, and X-band. The offered FSS is 26 cm × 26 cm and contains 676 unit cells. The design of the unit cell consists of a hexagonal loop and an irregular decagonal loop on the front side of the FR4 substrate, and a square loop with four annular rings attached to its corners on the backside. The rejected frequency ranges are from 2.3-4 GHz, 5-6 GHz, and 8-12 GHz. A prototype of the proposed design was manufactured in size of 26 cm × 26 cm and tested in the laboratory. Measured results for TE polarization and TM polarization at variant angles of incidence verify the simulation results and show the merits of the proposed design. The advantages of the proposed FSS are compactness, simplicity, wideband design, which makes it a convenient option for use as a stop-band filter.

TABLE II. Comparison with similar structures to demonstrate the advantages of the proposed design.

Reference	Unit cell size(mm^3)	Num. of bands	Bandwidth (GHz)	Substrate	Num. of substrate	Polarization independence	802.16d WiMAX	802.16e WiMAX	Bluetooth 802.11 WLAN	Bluetooth	X-band
[5]	10 × 10 × 1.6	3	3.2-3.7, 4.1-6, and 8-12.1	FR4	1	×	✓	×	✓	×	✓
[7]	10 × 10 × 1.6	1	4.6-16	FR4	1	×	×	×	✓	×	✓
[18]	20 × 20 × 1.6	3	1.4-1.9, 2.4-2.6, and 3.2-4.1	FR4	1	✓	✓	✓	×	✓	×
[19]	15 × 15 × 1.5	1	2.7-13.2	FR4	2	✓	✓	×	✓	×	✓
[20]	5 × 5 × 0.5	1	1-4	FR4	1	×	×	✓	✓	✓	×
[21]	9 × 9 × 1.6	1	3-7	FR4	1	✓	✓	×	✓	×	×
[22]	25.2 × 25.2 × 0.5	3	1.9-2.7, 5-5.37, 5.8-6.1	Rogers 4003c	1	✓	×	✓	✓	✓	×
[23]	8 × 8 × 0.5	1	3.9-8	F4BM220	2	✓	✓	×	✓	×	×
[24]	36 × 36 × 1.6	5	0.6-1.1, 1.49-1.51, 1.7-2.08, 3.4-3.58, 5.3-6.15	FR4	1	✓	✓	×	×	×	×
Proposed FSS	10 × 10 × 1.6	3	2.3-4, 5-6, and 8-12	FR4	1	✓	✓	✓	✓	✓	✓

REFERENCES

[1] K. K. Varikuntla and R. Singarav, "Review on Design of Frequency Selective Surfaces based on Substrate Integrated Waveguide Technology", *AEM*, vol. 7, no. 5, pp. 101–110, Nov. 2018.

[2] A. Kapoor, R. Mishra, and P. Kumar, "A Compact High Gain Printed Antenna with Frequency Selective Surface for 5G Wideband Applications", *AEM*, vol. 10, no. 2, pp. 27–38, Jul. 2021.

[3] B. Döken & M. Kartal, "Dual-band Frequency Surface Design by Implementing a Simple Design Technique", *IETE Journal of Research*, (2019), DOI: 10.1080/03772063.2019.1684848

[4] B. A. Munk "Frequency Selective Surfaces: Theory and Design". New York, *Wiley-Interscience*, 2000.

[5] M. Bashiri, Ch. Ghobadi, J. Nourinia, et al., "WiMAX, WLAN, and X-Band Filtering Mechanism: Simple-Structured Triple-Band Frequency Selective Surface". *IEEE Antennas and wireless propagation letters*. 2017; vol.16, p. 3245-3248.

[6] M. Majidzadeh, C. Ghobadi, J. Nourinia, "Quadruple filtering mechanism through an effective sketch of reconfigurable frequency selective surface". *Microw. Antennas Propag*. 2016; vol. 10, no.16, p. 1605–1612.

[7] M. Majidzadeh, C. Ghobadi, J. Nourinia, "Ultrawideband electromagnetic shielding through a simple single-layer frequency selective surface". *Wireless Pers. Commun*. 2017; vol. 95, p. 2769–2783.

[8] X.Xiong, W. Hong, Zh. Zhao, et al., "WiFi band-stop FSS for increased privacy protection in smart building". *2015 IEEE 6th International Symposium on MAPE*, Shanghai. 2015; p. 826-828.

[9] L.M. Araujo, R.H.C. Manicoba, A.L.P.S. Campos, A.G. D'assuncao, "A simple dual-band frequency selective surface*". Microwave and Opt Technol Lett*. 2009; vol. 51, p. 942-944.

[10] C.k.Lee, R.J. Langley, "Performance of a dual-band reflector antenna incorporating a frequency selective subreflector". Int J Electron 61. 1986; p. 607-616.

[11] J. H Kim., H. J. Chun, et al., "Analysis of FSS radomes based on physical optics method and ray tracing technique". *IEEE Antennas Wireless Propag. Lett*. 2014; vol. 13, p. 868-871.

[12] H. B.Baskey, B. Ghai, M. J. Akhtar. "A flexible ultra-thin, frequency selective-surface based absorber film for the radar cross-section reduction of a cubical object". *2015 IEEE MTT-S International Microwave and RF Conference (IMaRC)*, Hyderabad. 2015; p. 128-131.

[13] M.R.I. Faruque, M.M. Hasan, et al., "Tree-shaped fractal meta-surface with left-handed characteristics for absorption application". *Applied Physics A*. 2018; 124-127. https://doi.org/10.1007/s00339-017-1498-9

[14] A. Kesavan, M. Mantash, T.A. Dendini, "Supershaped reconfigurable frequency selective surfaces using cantilever enable switches". *Microw Opt Technol Lett*. 2019; p. 1-3. DOI: 10.1002/mop.31933

[15] BS. DA Silva, ALPS. Campos, N.A. Gomes, "Narrowband shielding against electro-magnetic interference in LTE 4G systems using complementary frequency selective surfaces". *Microw Opt Technol Lett*. 2018; vol. 60, p. 2293-2298. https://doi.org/10.1002/mop.31341

[16] S.Can, EU. Karakaya, AE. Yilmaz, "Design, fabrication, and measurement of textile-based frequency selective surfaces". *Microw Opt Technol Lett*. 2020; p. 1-7. https://doi.org/10.1002/mop.32474

[17] M.M. Hasan, M.R.I Faruque, T. Islam, "Dual band metamaterial antenna for LTE/Bluetooth/WiMAX system". *Scientific reports*. 2018; p. 8:1240. Doi:10.1038/S41598-018-19705-3

[18] Y.Garg, R. Chahar, et al., "A Novel polarization independent triple bandstop Frequency Selective Surface for the mobile and wireless communication". *International Conference on Computing, Communication and Automation (ICCCA)*, 2017; p. 1518-1521.

[19] H.F.Huang, Sh.F. Zhang, Y.H Hu, "A novel frequency selective surface for ultra-wideband antenna performance improvement", *In Proceedings of the international symposium on antennas & propagation (ISAP)*. 2013; p. 965–968.

[20] ZU. Abidin, Q. Cao, et al., "Design of a novel miniaturized bandstop frequency selective surface exhibiting polarization insensitivity and enhanced oblique stability". *Int J RF Microw Comput Aided Eng*. 2020; e22263. https://doi.org/10.1002/mmce.22263

[21] D. Belmessaoud, K. Roubah, et al.," Broadband planar slot antenna using a simple single-layer FSS stopband". *IET Microw. Antennas Propag.*, 2020; vol. 14 Iss. No. 3, p. 203-210. DOI: 10.1049/iet-map.2019.0365

[22] M. Karahan, E. Aksoy, "Design and analysis of angular stable antipodal F-type frequency selective surface with multi-band characteristics". *Int J RF Microw Comput Aided Eng*. 2020; e22466. https://doi.org/10.1002/mmce.22466

[23] W. Yu, G.Q. Luo, et al., "Miniaturised band-absorptive frequency selective rasorbers with wide absorption band". *IET Microw. Antennas Propag*. 2019; vol. 13 Iss. no.11, p.1777-1781. DOI: 10.1049/iet-map.2018.6170

[24] U. Farooq, A. Iftikhar, et al., "polarization insensitive Penta-bandstop frequency selective surface for closely placed bands". *Microw Opt Technol Lett*. 2020; p. 1-8. https://doi.org/10.1002/mop.32571

[25] Y. Jiaao, P. Shirui, et al., "Equivalent circuit model of an ultra-wideband frequency selective surface composite absorbing material". *J. Eng*. 2019; vol. 19, p.5922-5926. DOI: 10.1049/joe.2019.0220

[26] A. Ramezani, Z.H. Firuozeh, A. Ebadinezhad "Equivalent circuit model for array of circular loop FSS structures at oblique angles of incidence". *IET Microw. Antennas Propag.* 2018; vol. 12, p. 749-755. DOI: 10.1049/iet-map.2017.1004

[27] S. Keyrouz, G. Perotto, H.J. Vvisser "Lumped-Element Tunable Frequency Selective Surfaces". *The 8th European Conference on Antennas and Propagation IEEE*. 2014; p.475-478